2018 IEEE Conference on Decision and Control (CDC)
Miami Beach, FL, USA, Dec. 17-19, 2018

Impact of Solar Panels and Cooling Devices on Frequency Control after a Generation Loss Incident

Andrea Peruffo[1], Emeline Guiu[2], Patrick Panciatici[2] and Alessandro Abate[1]

Abstract— **Common household devices, such as solar panels and refrigerators, offer a considerable potential for frequency regulation, given their aggregate power generation and consumption. In this paper we present a simple approach to control the power contribution of a population of solar panels and thermostatically controlled loads, via a proportional control, in accordance with the current primary control practice. This control is suitable for a decentralized implementation. In addition, we consider the effect of renewables on the electricity network transfer function. We have tested the framework on a generation loss incident with different amount of solar power. Simulations display the capability of the control scheme and underline a chance of load shedding with a growing population of solar panels.**

I. INTRODUCTION

Renewable power has significantly increased its importance over the last decade. The energy market accommodates more and more solar, wind, thermal power [1] and their costs are becoming competitive [2]. Currently, solar energy is the fourth power source among renewables, with more than 100 TWh produced in the EU area in 2016 [1]. Renewable energy producers could, in principle, inject power into the grid but, in general, they do not participate in the regulatory action [3]. The intrinsic unpredictability, connected mainly to weather conditions or seasonal effects, remains an obstacle to the full deployment of this technology. An overview of the issues and main challenges on frequency regulation with the integration of renewable can be found in [4].

In this paper we present a continuous-time model for a large heterogeneous population of photovoltaic (PV) panels connected to the electric network. We develop a four-state Markov chain model, to encompass the PV device activation state (ON/OFF) and the frequency value. We assume that a single panel is equipped with an internal clock and can sense the network frequency signal. In order to be active, the local network frequency must be around the nominal value $f_0 = 50$ Hz. For safety reasons, a panel can only connect to a network that remains stable for a given amount of time, hence the need for the internal clock. Each panel of the population has heterogeneous frequency working interval and delay. In [5] and [6] we have built discrete-time Markov chain models for such a population, and have studied the effect of the dispersion of these two variables. Differently from our previous works, in this article we assume to control the output of single PV panels under a proportional control law, similarly to the primary control currently implemented by traditional synchronous machines.

Renewables influence the electric grid they are connected to. Typically, the moment of inertia of the electric network is considered constant. This assumption is well justified when solely synchronous machines are utilised. However, when the solar population has a significant contribution on the network, we need to consider its impact: we assume that solar panels have no inertia and we modify the grid transfer function accordingly. We study the root locus and analyse how solar panels modify the response of the electric network.

Alongside solar panels, we consider a population of thermostatically controlled loads (TCLs). Common such devices are fridge/freezers, coolers and air conditioning systems. We similarly employ a four-state Markov chain to the behaviour of a TCL device and use the same proportional control law for the aggregated population. Literature shows several examples of control of a TCLs population [7], [8], [9], [10] for flexible demand-response. Fridges are one of the most common electrical appliance and are potentially always active. Several studies have proved that their contribution to the global load is significant. Therefore, being able to control them can have benefits for frequency regulation. This can be seen as a frequency regulation at a household level: TCLs on the consumption side, panels on the generation side.

The aim of this work is to show how common devices can contribute to network stability with a simple proportional control scheme. More refined control methods are available, but we choose such a control design in order to be consistent with the present primary control [11]. However, the control action offered by the current primary control takes several seconds to operate. Inverter-driven devices can act virtually with no delay. Simulations provide evidence of the benefit that can arise from controlling these devices. Furthermore, they underline the impact of engaging PV panels without any regulatory action, supporting the analysis in [12].

The remainder of this paper is organized as follows: Section II presents continuous time models of solar panels and TCLs. Section III introduces an electric grid model with a dependence on the ratio between traditional power generated by synchronous machines and total consumption. In Section IV we present the control design, aligned to the network primary control framework, considering both PV panels and TCLs. Simulations are used to highlight the capability of these two populations to enhance the stability of the network after an infeed loss incident. Finally, conclusions are drawn in Section VI.

[1]Andrea Peruffo and Alessandro Abate are with the Department of Computer Science, University of Oxford, OX1 3QD, United Kingdom name.surname@cs.ox.ac.uk

[2] Emeline Guiu and Patrick Panciatici are with Réseau de Transport d'Électricité France, 78000, Versailles name.surname@rte.com

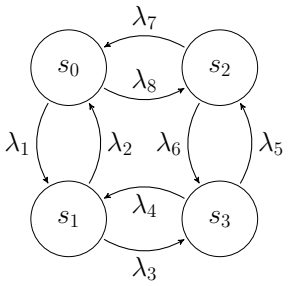

Fig. 1. Markov chain representation of the population. States s_0, s_1 represent mode ON, whereas s_2, s_3 mode OFF. States s_0, s_2 represent $f(\cdot) \in \mathscr{I}_f$, whereas s_1, s_3 $f(\cdot) \notin \mathscr{I}_f$.

II. MODELS

A. Photovoltaic panels

A description of models for photovoltaic panels connected to the electric network can be found in literature [5]. We report here a brief version for completeness. In this work, we consider household devices installed on home roofs. A population of such devices is prone to heterogeneity, due to different manufacturers, ages, weather conditions, etc. Panels are connected to the electrical grid and sample its frequency. A panel can be either ON or OFF. The switching among these two states depends on two quantities: the network frequency $f(\cdot)$ and a safety time delay τ_r. Regulations impose the panel to work (state ON), solely when the grid frequency $f(\cdot)$ belongs to the interval $\mathscr{I}_f = [f_{uf}, f_{of}]$, a neighbourhood of the nominal frequency f_0. If the frequency exits $\mathscr{I}_f$, the panel must disconnect (state OFF). We consider the ON-to-OFF transition to be very fast; it should be taken as soon as $f(\cdot) \notin \mathscr{I}_f$. A solar panel only connects to a *supposedly stable* network: the network is considered to be stable if the frequency lies within $\mathscr{I}_f$ for a predefined amount of time, τ_r. The panel is equipped with an internal clock $\tau(\cdot)$. It is then compared to the time threshold τ_r, so that when $\tau(\cdot) \geq \tau_r$ the panel will turn ON if $f(\cdot)$ has remained within $\mathscr{I}_f$. Notice that if the frequency signal exits the interval $\mathscr{I}_f$, the counter is reset and the panel must wait again τ_r time instants to turn ON. The power generation can happen solely when the device is in state ON.

Drawing inspiration from [7] and from our previous work [5], [6] we present a continuous-time model for a population of PV panels. Given the coupling between ON/OFF and the network frequency, we include these two dynamics in our modeling framework. The design is therefore a four-state Markov chain, shown in Table I.

TABLE I

ENCODING OF STATES OF THE MODEL.

State Encoding	Activation	Frequency
s_0	ON	$f(\cdot) \in \mathscr{I}_f$
s_1	ON	$f(\cdot) \notin \mathscr{I}_f$
s_2	OFF	$f(\cdot) \in \mathscr{I}_f$
s_3	OFF	$f(\cdot) \notin \mathscr{I}_f$

Possible transitions are depicted in Fig. 1. States s_0, s_1 represent mode ON, whereas s_2, s_3 mode OFF. States s_0, s_2 represent the scenario $f(\cdot) \in \mathscr{I}_f$, whereas s_1, s_3 the scenario $f(\cdot) \notin \mathscr{I}_f$. We denote transition rates with λ_i. Rates λ_1 and λ_2 are rates connected to the variation of the grid frequency – if $f(\cdot) \in \mathscr{I}_f$ or not – while the device remains ON; analogously rates λ_5 and λ_6 when the device is OFF. Rates λ_7 and λ_8 indicate the rates of switching between ON and OFF while the frequency remains within $\mathscr{I}_f$; similarly for λ_3 and λ_4 when $f(\cdot) \notin \mathscr{I}_f$. The physical description imposes a limitation to our model: $\lambda_2 = 0 = \lambda_4$ for all values of $f(\cdot)$. This reflects the fact that once a panel senses the frequency outside its working interval, it must turn OFF. The behaviour of the panels also suggests that the other rates depend on the grid frequency. Intuitively, as the frequency deviation $\Delta f(t) = f(t) - f_0,\ t \geq 0,\ t \in \mathbb{R}$ increases, the probability of switching OFF increases.

The population of solar panels is heterogeneous, therefore the working interval $\mathscr{I}_f$ is inhomogeneous across the population. Instead of a single value of disconnection and reconnection threshold, we consider a *distribution* of thresholds. We introduce a shift in perspective: from a single panel with deterministic thresholds to a population of devices with a probability of switching. Here, the probability of being in a state represents the portion of devices being in that state. In order to describe the switching of the heterogeneous population model, we assume to know the distribution of thresholds across the devices. Let us define $p_{u,d}(\cdot)$, $p_{o,d}(\cdot)$, $p_{u,r}(\cdot)$ and $p_{o,r}(\cdot)$ to be the probability distribution of thresholds; here the subscript u stands for under-frequency, o over-frequency, d disconnection, r reconnection. We formulate the dependency of rates from the frequency deviation as

$$\lambda_i(f(t)) = \lambda_i^0 + w_{i,j} \int_0^{\Delta f(t)} p_j(u)du,\ i = 1, \dots 8,$$

where $\lambda_i^0 \geq 0$ represents the rates at $f(t) = f_0$, $j \in \{(u,d),(u,r),(o,d),(o,r)\}$, and $w_{i,j}$ is a weighting constant. Clearly, $\lambda_1, \lambda_3, \lambda_5, \lambda_7$ relate to reconnection, whereas $\lambda_2, \lambda_4, \lambda_6, \lambda_8$ to disconnection. Note that we assume to have no control on the rates. Denote $\pi_i(t)$ as the probability of being in state i at time t. Equations of the probability evolution in time are written as the system equations

$$\begin{cases} \dot{\pi}_0(t) = -(\lambda_1 + \lambda_8)\pi_0(t) + \lambda_2\pi_1(t) + \lambda_7\pi_2(t) \\ \dot{\pi}_1(t) = \lambda_1\pi_0(t) - (\lambda_2 + \lambda_3)\pi_1(t) + \lambda_4\pi_3(t) \\ \dot{\pi}_2(t) = \lambda_8\pi_0(t) - (\lambda_6 + \lambda_7)\pi_2(t) + \lambda_5\pi_3(t) \\ \dot{\pi}_3(t) = \lambda_3\pi_1(t) + \lambda_6\pi_2(t) - (\lambda_4 + \lambda_5)\pi_3(t) \end{cases} . \quad (1)$$

For convenience, we define also $\pi_{ON} = \pi_0 + \pi_1$ and $\pi_{OFF} = \pi_2 + \pi_3$. From standard Markov chain theory [13], it can be proved that this system has a unique stationary distribution, denoted $\bar{\pi}_i,\ i = 0 \dots 3$. We consider the power production $P(t)$ to be directly proportional to the probability π_{ON} of being in state s_0 or s_1. Furthermore, we add a white Gaussian noise $\sigma_{PV}(t)$ to account for weather uncertainties, the heterogeneity of the population, etc. Formally,

$$P(t) = \bar{P}\pi_{ON}(t) + \sigma_{PV}(t), \quad (2)$$

where $\bar{P}$ is the constant power generation of the single PV panel. This is a reasonable assumption over small time scales

(seconds) and during a clear day. However, this assumption might not hold under an overcast sky: individual solar plants can significantly vary their outputs within few seconds [14].

B. Thermostatically Controlled Loads

Thermostatically controlled loads (TCLs) consist of an electrical heating or cooling element, controlled by a thermostat. Their aim is to maintain the temperature within an interval, which is commonly achieved via hysteresis control. In the following we refer to cooling systems, specifically to refrigerators. Literature shows great interest in analysis and control design for frequency regulation without affecting the final user. In [15] devices monitor the frequency deviations and adjust their power consumption accordingly. More recently [16] a similar idea is discussed for cooling units over the British network. Only considering refrigerator/coolers in GB, the population is around 20 millions devices [17], each consuming from 100 to 400 W. In [7] a two-state model for dynamic demand management of refrigerators is presented. The authors design a random controller to cope with power outages and to avoid devices synchronization. In [8] a decentralized control of a heterogeneous population of TCLs is utilised to follow a reference power profile for flexible demand-response framework. In [9] the authors prove that a control on the temperature of a population of fridges is not reliable in terms of network stability. They instead propose a control on the power consumed based on the frequency deviation.

We consider a similar model for PV panels to be valid also for TCLs. Our modeling framework is based on the following assumptions, as an implementable and plausible behaviour. A single device samples the frequency and detects whether this is inside or outside a pre-defined interval $\mathscr{I}_f$. If the frequency lies outside the interval, the device re-samples the frequency after a random delay. If the frequency is measured outside $\mathscr{I}_f$, the device turns OFF. When the device is OFF, it must wait until the frequency returns within the interval $\mathscr{I}_f$. The random delay prevents synchronization issues that might enhance network instability. With this design, a device can be depicted as a four-state Markov chain, as shown in Fig. 1. Note that $\lambda_2, \lambda_4 \neq 0$, since refrigerators do not have the same limitations as solar devices. Similarly to panels, $\pi_i(t), i = 0 \dots 3$ represents the probability of being in state i at time t. Recall that $\pi_{ON}(t) = \pi_0(t) + \pi_1(t)$: this value relates to the duty cycle of a device. We now briefly discuss the temperature evolution of TCLs (for a more complete analysis, please refer to [8]). Every TCL has an inner temperature variable T that evolves as

$$\dot{T} = \begin{cases} \alpha(T_{off} - T) & when\ OFF\ (states\ s_2, s_3) \\ -\alpha(T - T_{on}) & when\ ON\ (states\ s_0, s_1) \end{cases}, \quad (3)$$

where α is constant and T_{on}, T_{off} are asymptotic temperatures for the ON and OFF states. The temperature of a single device must remain within the interval $[T_{min}, T_{max}]$. In the following we assume to control the switching between ON and OFF by varying the rates of the Markov chain. The power consumption $P(t)$ is assumed to be directly proportional to the probability of being in state s_0 or s_1. We consider a white Gaussian noise $\sigma_L(t)$ to model the heterogeneity of the TCL population. Formally

$$P(t) = -\bar{C}\pi_{ON}(t) - \sigma_L(t),$$

where $\bar{C}$ represent a constant power consumption of a single cooling unit. The power equation is analogous to (2), noting that the negative sign represents power consumption rather than power generation.

III. GRID STRUCTURE

Models of the national or European grid [18] are strictly linked to the concepts of synchronous machines and inertia. Traditionally, when considering synchronous machines, the total moment of inertia of the network is modelled as a constant. Renewable power sources however do not follow this assumption: solar panels have no moving parts, which implies no mechanical inertia at all. If the solar irradiance is blocked, the solar devices immediately stop generating electricity. The contrary is also true: when the sun shines, power is generated immediately. To encompass the dual nature of power sources we write the transfer function of the network as a function of the amount of conventional power generated by synchronous machines. The transfer function in (4) we utilize is of second order and derived from [19]. We assume a linear relation between T_L, the time to launch (related to the inertia of the system), and the amount of conventional power generated in the network. Intuitively, the more generators in the network the more inertia governs the frequency evolution; therefore the starting time increases. Formally, we use $T_L = \frac{CP}{k_T}$, where $CP \geq 0$ represents the conventional power and k_T is a constant value. Note that in case of $CP = 0$ we obtain $T_L = 0$. We will not discuss this issue here, as it is out of the scope of this work. We obtain a transfer function as a function of CP:

$$G(s, CP) = \frac{(s+1)}{\frac{CP}{k_T}s^2 + \left(k_a + \frac{CP}{k_T}\right)s + (k_a + k_{PU})}. \quad (4)$$

Notice that k_{PU} is inversely proportional to S, the total load in the network and $S \geq CP$, where the equality represents a network without any renewable power.

A. Root Locus

We study how the ratio CP/S influences the stability of the network. The standard technique [20] of the root locus analysis is employed. We utilise a proportional control, as explained in Section IV, under different percentage of CP/S. Fig. 2 shows the root locus in three different conditions: $CP/S = 1$ (no renewables), $CP/S = 0.8$ and $CP/S = 0.5$, with $S = 80$ GW. The more renewable power, the more oscillatory the system becomes, which leads to bigger overshoots. We notice that also the real part increases in absolute value, meaning a faster convergence to zero. However, wider oscillations could eventually cause issues in the electric grid setting. The grid operators should avoid wide variations of the frequency signal, as this brings the network to its operational limits and may cause load shedding.

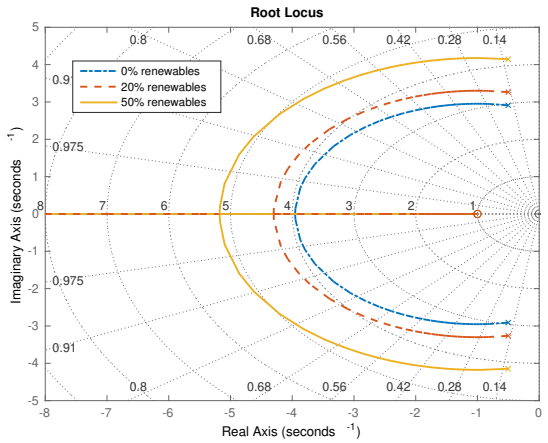

Fig. 2. Root locus with just traditional power sources (blue solid line), 20% (red dashed) and 50% (yellow dotted) renewable power.

IV. CONTROL DESIGN

The operation mode of PV panels is crucially determined by the so called Maximum Power Point Tracking (MPPT) algorithm. In this work we assume to be able to control the power output at a single device level via a proportional gain. We argue that this idea can be implemented in the inverter alongside the MPPT algorithm with little effort. Once the algorithm finds the MPP, it can compute the desired power output via the proportional control, and chooses the new working point. We propose a decentralized design to control the population of PV panels. We assume that each device, during normal operations, injects P_0 power into the grid, strictly less than the maximum available power P_{MAX}. P_0 can be tuned according to requirements by the Transmission System Operator [21]. We set P_0 to represent 90% P_{MAX}. We utilise a proportional control law such as

$$P(t) = P_0 + k_p \cdot \Delta f(t), \tag{5}$$

where $P(t)$ represents the instantaneous power injection, k_p is a constant gain, and $\Delta f(t) = f(t) - f_0$ represents the frequency deviation from the nominal value.

The value k_p is computed taking into account the disturbance rejection at steady state d_{ss} in case of a step disturbance $d(t) = A > 0,\ t \geq 0$, so that

$$d_{ss} = A \cdot \frac{G(0,\overline{CP})}{1 + k_p G(0,\bar{CP})},$$

where $G(0,\overline{CP})$ is the steady state gain of $G(s,CP)$ with a constant value of CP. Assuming a maximum steady state disturbance value d_{ss}^{max}, we can characterise a working region

$$k_p \geq G(0,\overline{CP})^{-1} \left(\frac{A \cdot G(0,\overline{CP})}{d_{ss}^{max}} - 1 \right).$$

We find a minimum value for k_p that is then compared to the root locus analysis in Section III, and depicted in Fig. 2.

Usually in power systems the control action presents a deadband, i.e. if the frequency is close enough to the nominal value f_0 no control action is needed. In case of underfrequency, we denote the interval in which the control act as $[f_u^{min}, f_u^{max}]$; similarly in case of overfrequency, $[f_o^{min}, f_o^{max}]$. Note that this interval is not related to the working thresholds of the devices, presented in Section II. The deadband approach is useful in real life applications, where the frequency signal is inevitably noisy causing the frequency to never settle on the nominal value. The control design linked to (5) is depicted in Fig. 3.

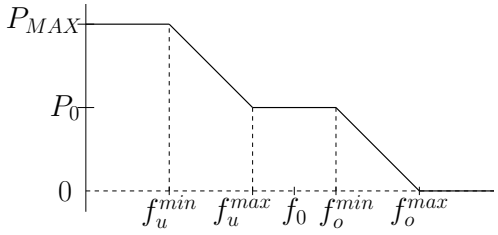

Fig. 3. Controlled power output of the population vs. network system frequency. P_0 is the set power at nominal conditions, P_{MAX} is the maximum power output in situation of underfrequency. If the frequency increases, the power output can go to zero.

Once the proportional gain k_p for solar devices is found, we utilize a similar approach also for the control of the duty cycle π_{ON}^L. We use superscripts $\cdot^L$ and $\cdot^{PV}$ to indicate TCL and solar devices quantities, respectively. In Section II we have defined the power consumption at time t of the TCL aggregation as directly proportional to $\pi_{ON}^L(t)$. We recall from standard Markov chain [13] theory that $\pi_i(t)$ exponentially tends to $\bar{\pi}_i$, the steady state distribution. Recalling (2) and (5), we impose that $\bar{\pi}_{ON}^L$ equals to the desired power output as

$$\bar{\pi}_{ON}^L(t) = \bar{\pi}_{ON}^{L,0}(t) + \frac{k_p \cdot \Delta f(t)}{\bar{C}},$$

where $\bar{\pi}_{ON}^{L,0}(\cdot)$ represents the duty cycle when the frequency is around f_0. From $\bar{\pi}_{ON}^L$ the other elements in vector $\bar{\pi}^L$ are derived. Notice that in nominal conditions $f(t) = f_0$, hence $\pi_1(t) = 0 = \pi_3(t)$, $\pi_{ON}(t) = \pi_0(t)$ and $\pi_{OFF}(t) = \pi_2(t)$. We saturate the value of π_i so that $\pi_i(t) \in [0,1],\ \forall t$.

The purpose is to make the TCL population converge to the desired power consumption π_{ON}^L. The steady state condition is imposed modifying the rates in infinitesimal generator matrix Q (see e.g. [13]) solving

$$[\bar{\pi}_0^L\ \bar{\pi}_1^L\ \bar{\pi}_2^L\ \bar{\pi}_3^L] \cdot Q(t) = 0. \tag{6}$$

We assume to modify the rates λ_i^L in order to have rates as function of the network frequency: $\lambda_i^L = \lambda_i^L(f(t)),\ \forall i$. Equation (6) has five degrees of freedom, so we can control five λ_i^L: we choose a proportional law to update the rates as

$$\lambda_i^L(f(t)) = \lambda_i^{L,0} + k_i \Delta f(t),$$

where $\lambda_i^{L,0} \geq 0$ is the value of λ_i^L at $f(t) = f_0$.

V. SIMULATION RESULTS

In this section we utilize the developed models and control to illustrate the response after an incident in several scenarios. In line with the ENTSO-E requirements [19] we simulate

an infeed loss of 3 GW in a global network demand $S = 80$ GW. The network model parameters are chosen according to the values used in [19], i.e. $k_a = 0.01$, $k_{PU} = 15 \cdot 10^3$, $T_L = CP/k_T$, $k_T = 15 \cdot 10^3$. Power and frequency values are normalised (per unit) relative to S and to 50 Hz.

The effect of the populations of panels and TCLs is examined through simulation of the equivalent of 20 millions TCLs and three different contributions of PVs. Solar aggregation is set to represent the 10%, 20% and 40% of S, representing a population of $3 \cdot 10^6$, $6 \cdot 10^6$ and $12 \cdot 10^6$ panels, respectively. Power consumption of a single TCL $\bar{C}$ is set to 200 W, a single panel generation $\bar{P}$ to 3 kW. The variance of σ_{PV} and σ_L are set to 1% of $\bar{P}$ and $\bar{C}$, respectively. The model parameters for the TCL population are derived from [9]: $\alpha = 1.37 \cdot 10^{-4} s^{-1}$, $T_{on} = -44°C$, $T_{off} = 20°C$, $T_{min} = 2°C$, $T_{max} = 7°C$. Initial rates values are $\lambda_1^{L,0} = 0$, $\lambda_2^{L,0} = 2.5$, $\lambda_3^{L,0} = 12.5$, $\lambda_4^{L,0} = 2.5$, $\lambda_5^{L,0} = 2.5$, $\lambda_6^{L,0} = 0$, $\lambda_7^{L,0} = 1$, $\lambda_8^{L,0} = 3$. These values are computed in order to represent a population with duty cycle $\pi_{ON}^{L,0}$ around 25%. Temperatures of the population are updated singularly as in (3), and temperatures are updated according to the following. Whenever the temperature of a single refrigerator reaches T_{min}, the device is forced to remain OFF – so the temperature to increase – until $T = T_{min} + 1°$. On the other side, when the temperature reaches T_{max}, the device is turned ON until the temperature equals $T_{min} + 1°$. This mechanism overrides the control of λ_i^L $\forall i$, in order to comply with the temperature specifications. Regarding the PV population, we utilise a χ^2 distribution as in [6] for the under- and over- frequency thresholds. We assume to have a given proportion of panels that are activated according to the regulation shown in Table II. We assume also that the condition to comply with the regulations is to have a threshold equal to the limit or further away from f_0. E.g., panels installed with the 49.5 Hz underfrequency limit can have a threshold $f_{uf} \leq 49.5$ and similarly for overfrequency. Panels rates λ_i^{PV} are computed integrating the χ^2 distributions, using initial values $\lambda_1^{PV,0} = 0$, $\lambda_2^{PV,0} = 0$, $\lambda_3^{PV,0} = 2.5$, $\lambda_4^{PV,0} = 0$, $\lambda_5^{PV,0} = 2.5$, $\lambda_6^{PV,0} = 0$, $\lambda_7^{PV,0} = 10^{-2}$, $\lambda_8^{PV,0} = 0$. Controllers utilise a frequency deadband (see Fig. 3) $[f_u^{max}, f_o^{min}] = [49.95, 50.05]$ Hz. We assume every panel implements the same proportional control design, with $k_p = 4$. The same value is utilised to compute the desired duty cycle $\bar{\pi}_{ON}^L$. The rates update utilises $k_i = 0.5$ $i = 1, 2, 5, 7$ and $k_3 = -0.5$; $\lambda_4, \lambda_6, \lambda_8$ are obtained as a function of the previous ones. Rates are then saturated at a minimum value of zero, i.e. $\lambda_i(f(t)) \in [0, +\infty)$, $\forall i$. Simulations are implemented using MATLAB software. The grid frequency is sampled at a rate of 0.2 s, consistently with requirements introduced in [3], both for panels and TCLs. The discussion is focused on the consequences of an incident after few seconds: the simulation time is set to $20s$.

A. Results

This study aims at highlighting the hidden capabilities of common devices as refrigerator and solar panels to help sustain the grid after an incident. The attention is directed mainly towards the load shedding value, happening at values of frequency below 49.2 Hz. We do not design any load shedding mechanism but simply check whether the frequency response crosses that value.

TABLE II
PARTITION OF UNDERFREQUENCY AND OVERFREQUENCY THRESHOLDS AND ASSOCIATED PORTION OF POPULATION.

Underfrequency threshold	49.8	49.7	49.5	49.0	47.5
Overfrequency threshold	50.2	50.2	50.2	50.2	50.2
% population	5	10	22.5	20	42.5

Fig. 4 depicts the frequency response after the infeed loss without any controlled device (solid line), with controlled TCLs (dashed), controlled PVs (triangle) and both controlled (dotted). Solar panels are set to contribute for 10% of the total load. Trivially, PVs give the most to the control action, having more power to inject in the network when needed. All the simulated scenarios get to the first threshold (49.8 Hz), when panels begin to turn OFF. All the simulations carry a steady state error due to the proportional nature of the control. Notice that the controlled TCLs scenario does not reach the second threshold (49.7 Hz), which would enable another portion of panels to turn OFF. An interesting response of the system is shown in Fig. 5. The non controlled and the controlled TCLs simulations reach a value of frequency that is lower than the previous simulation. The higher solar penetration (20%) causes more panels to trip at 49.8 Hz and at 49.7 Hz, leading to a bigger undershoot in the frequency response. We have more PV power to control, leading to less undershoot and the minimization of incident effects. Finally, Fig. 6 shows a more extreme situation, with solar at 40%. When the frequency trips 49.8 Hz panels start to disconnect, making the frequency decrease. This leads to the disconnection of more panels, causing a sudden drop in the frequency response. Under the controlled solar panels scenario, we notice an oscillatory behaviour. When the frequency signal exits the controller deadband, the proportional gain brings it back to a value closer to f_0, where the proportional gain drops to zero. The oscillation width depends upon the width of the deadband.

Our experiments underline the importance and the fragility of new power sources. Even if their contribution to the frequency response is not major, controlling simple appliances as refrigerators avoids greater undershoots that lead to more risky situations for the grid. Solar panels have a great potential and having them only subjected to the electric network can have a negative impact on the network stability.

VI. CONCLUSIONS

In this paper, we have introduced a continuous-time model for solar panels and adapted it to fit a possible implementation of TCLs. The four-state Markov chain exploits the delayed nature of the devices and encompasses the feedback connection between devices and grid network. Alongside, we have analysed how renewables impact the electric grid. We have utilised a linear relation to describe the dependency

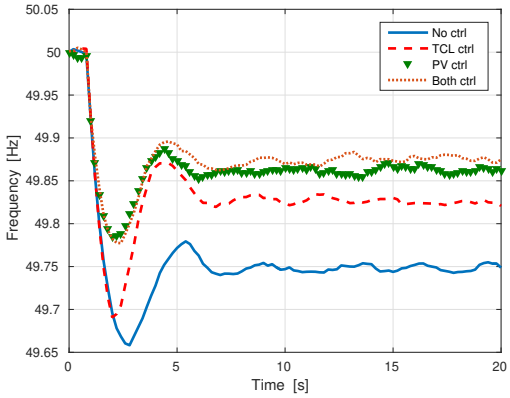

Fig. 4. Frequency responses with 10% solar: no control (solid line), controlled TCLs (dashed), PVs controlled (triangle), both population controlled (dotted).

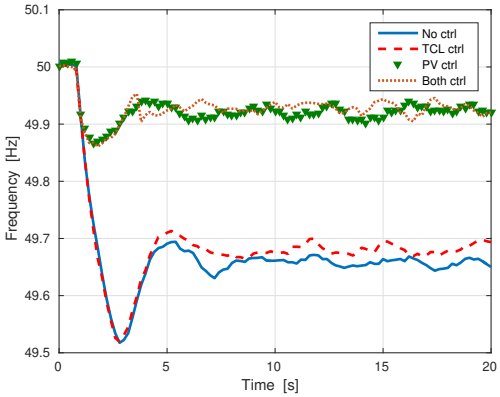

Fig. 5. Frequency responses with 20% solar: no control (solid line), controlled TCLs (dashed), PVs controlled (triangle), both population controlled (dotted).

between the amount of conventional power and network's time to launch. Under these assumptions, the introduction of renewables increases the oscillatory response of the grid after an incident. Wider overshoots are a dangerous inconvenience, as they can stress the physical network and potentially activate a load shedding procedure. Finally we have introduced a control scheme for controlling the aggregate populations of solar panels and TCLs. Panels individually adjust their power output and TCLs modify their duty cycle in order to enhance the stability of the electric grid following an incident. The control framework permits a decentralized implementation. This control design is simple but chosen in order to trace the already existing primary frequency control. Solar power without storage is clearly not reliable to serve as primary control. However, it can support the network in case of sudden losses, as demonstrated in this work. Simulations have proved the potential that is hidden in these common devices. We have tested a generation loss incident under three renewable penetration scenarios, verifying the effectiveness of such a simple controller design. They have also demonstrated how the panels disconnection behaviour can lead to load shedding, even if the current primary control is active.

REFERENCES

[1] ENTSO-E, "Statistical Factsheet," Tech. Rep., 2016.

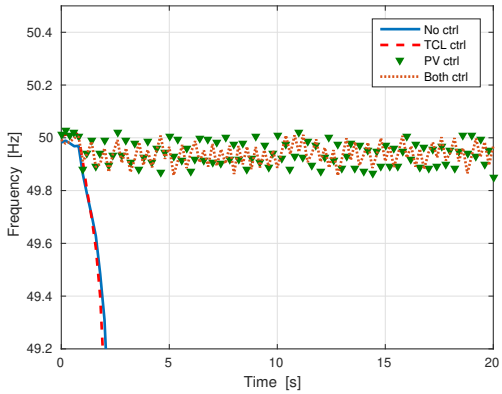

Fig. 6. Frequency responses with 40% solar: no control (solid line), controlled TCLs (dashed), PVs controlled (triangle), both population controlled (dotted).

[2] A. Griffin, "Solar and wind power cheaper than fossil fuels for the first time," http://www.independent.co.uk/environment/, 4 January 2017.
[3] E. Commission, "Commission Regulation (EU) 2016/631 of 14th April 2016," Tech. Rep., 2016.
[4] H. Bevrani, A. Ghosh, and G. Ledwich, "Renewable Energy Sources and Frequency Regulation: Survey and New Perspectives," *IET Renewable Power Generation*, vol. 4, no. 5, pp. 438–457, 2010.
[5] A. Peruffo, E. Guiu, P. Panciatici, and A. Abate, "Aggregated Markov Models of a Heterogeneous Population of Photovoltaic Panels," *International Conference on Quantitative Evaluation of Systems*, pp. 72–87, 2017.
[6] ——, "Synchronous Frequency Grid Dynamics in the Presence of a Large-scale Population of Photovoltaic Panels," in *Power Systems Computation Conference (PSCC), 2018*. IEEE, 2018.
[7] D. Angeli and P.-A. Kountouriotis, "A Stochastic Approach to 'Dynamic-Demand' Refrigerator Control," *IEEE Transactions on Control Systems Technology*, vol. 20, no. 3, pp. 581–592, May 2012.
[8] S. H. Tindemans, V. Trovato, and G. Strbac, "Decentralized Control of Thermostatic Loads for Flexible Demand Response," *IEEE Transactions on Control Systems Technology*, vol. 23, no. 5, Sept 2015.
[9] ——, "Frequency Control Using Thermal Loads Under the Proposed ENTSO-E Demand Connection Code," in *2015 IEEE Eindhoven PowerTech*, June 2015, pp. 1–6.
[10] S. E. Z. Soudjani and A. Abate, "Aggregation and Control of Populations of Thermostatically Controlled Loads by Formal Abstractions," *IEEE Transactions on Control Systems Technology*, vol. 23, no. 3, pp. 975–990, 2015.
[11] ENTSO-E, "Network Code on Operational Security," Tech. Rep., 2013.
[12] ——, "Assessment of the System Security with Respect to Disconnection Rules of Photovoltaic Panels," Tech. Rep., 2012.
[13] C. Baier and J.-P. Katoen, *Principles of model checking*, 2008.
[14] J. G. Kassakian, R. Schmalensee, G. Desgroseilliers, T. D. Heidel, K. Afridi, A. Farid, J. Grochow, W. Hogan, H. Jacoby, and J. Kirtley, "The future of the Electric Grid," *Massachusetts Institute of Technology, Tech. Rep*, pp. 197–234, 2011.
[15] F. C. Schweppe, "Frequency adaptive, Power-energy Re-scheduler," Feb. 23 1982, uS Patent 4,317,049.
[16] J. A. Short, D. G. Infield, and L. L. Freris, "Stabilization of Grid Frequency through Dynamic Demand Control," *IEEE Transactions on power systems*, vol. 22, no. 3, pp. 1284–1293, 2007.
[17] J. Hulme, A. Beaumont, and C. Summers, "Energy Follow-up Survey 2011. Report 9: Domestic Appliances, Cooking & Cooling Equipment," 2013.
[18] D. Jones, "Dynamic System Parameters for the National Grid," *IEE Proceedings - Generation, Transmission and Distribution*, vol. 152, no. 1, pp. 53–60, Jan 2005.
[19] ENTSO-E, "Policy 1: Load-frequency Control and Performance," Tech. Rep., 2009.
[20] R. C. Dorf and R. H. Bishop, *Modern Control Systems*, 2011.
[21] E. Commission, "Commission regulation (EU) 2017/1485 of 2 August 2017," Tech. Rep., 2017.